

ACS Macro Lett. Author manuscript; available in PMC 2014 August 20.

Published in final edited form as:

ACS Macro Lett. 2013 August 20; 2(8): 725-730. doi:10.1021/mz400331w.

# Block copolymers containing a hydrophobic domain of membrane-lytic peptides form micellar structures and are effective gene delivery agents

**Joan G. Schellinger**, **Joshuel A. Pahang**, **Julie Shi**, and **Suzie H. Pun**\*

Department of Bioengineering and Molecular Engineering & Sciences Institute, University of Washington, 3720 15<sup>th</sup> Ave NE, Box 355061, Seattle, Washington 98195, United States

### **Abstract**

Endosomal release peptides have been incorporated in synthetic gene delivery formulations to increase transfection efficiencies. In this work, cationic copolymers containing sHGP, a membrane-lytic peptide derived from HIV gp41, were synthesized and evaluated. Diblock, with sHGP displayed on one block, and statistical, with sHGP randomly displayed, copolymers were prepared via RAFT polymerization. While the statistical copolymer existed as unimers in solution, amphiphilic diblock copolymers self-assembled into cationic micelles in aqueous solution as evidenced by TEM and dynamic light scattering analyses. This self-assembly sequestered the lytic domain and significantly reduced the cytotoxicity of the materials. However, when complexed with plasmid DNA, both the diblock and statistical copolymers of sHGP showed higher gene delivery efficacy compared to the copolymers without the membrane lytic motif. The ability of amphiphilic, diblock copolymers containing endosomal release motifs to self-assemble and sequester lytic domains is a promising feature for the nucleic acid delivery.

Endosomal release and cytosolic delivery of therapeutics still remains a major barrier in achieving an efficient nonviral nucleic acid therapy. Macromolecular cargos that enter cells by endocytosis will become inactivated in lysosomal compartments unless released from this degradatory pathway. Thus, recent developments in nucleic acid delivery include the development of multifunctional vehicles that can overcome barriers such as endosomal escape. These biomaterials enable productive delivery of genes and oligonucleotide therapeutics to mammalian cells. <sup>2,3</sup>

Peptides are a promising class of bioactive molecules that can be easily functionalized and incorporated into polymeric systems. Membrane-active peptides such as melittin or INF7 have been adapted as endosomal release peptides in intracellular delivery formulations. The use of these and other peptides in gene delivery vehicles was reviewed recently. These bioactive peptides are incorporated for nucleic acid complexation, as targeting ligands, and to overcome entrapment from the endocytic pathway. Peptides can therefore function as key components of delivery vectors by facilitating efficient gene expression. Previously, we reported a 15-amino acid peptide, sHGP, derived from the endodomain of HIV gp41, that displays membrane-lytic ability. <sup>6,7</sup> Conjugation of sHGP to branched polyethylenimine (PEI) led to enhanced transfection efficiency compared to unmodified PEI and scrambled sHGP-modified PEI. However, disadvantages of using PEI-based materials *in vivo* include

<sup>\*</sup>Corresponding Author. spun@u.washington.edu.

their lack of degradability, their propensity to induce erythrocyte aggregation, and their ability to activate the complement cascade. 9,10

Herein, we report the incorporation of sHGP into a peptide-based polymeric system composed of oligopeptide monomers ( $K_{10}$ ) (for nucleic acid binding) and N-(2-hydroxypropyl)methacrylamide (HPMA) in two different architectures. We utilize a modular synthesis involving reversible addition-fragmentation chain transfer (RAFT) polymerization that allows us to incorporate different bioactive peptides, such as endosomal escape peptides, in a block 12 or statistical 13 form. Polymerization via the RAFT method offers advantages in preparation of polymers with narrowly-dispersed molecular weights and well-defined composition and structure for gene transfer.  $^{14,15}$ 

Statistical copolymers containing sHGP (st-sHGP) were prepared by copolymerization of HPMA, methacrylated-*oligo-L*-lysine (MaAhxK<sub>10</sub>) and methacrylated-K<sub>3</sub>-sHGP (MaK<sub>3</sub>sHGP) using a trithiocarbonate-based chain transfer agent in a 2:1 acetate buffer / ethanol solvent mixture (Scheme1A). The monomer feed ratio and the degree of polymerization was chosen based on our previous optimization studies: 77% HPMA, 20% MaAhxK<sub>10</sub>, 3% MaK<sub>3</sub>sHGP at degree of polymerization (DP) of 190. Three lysine residues were included as a linker in the methacrylamido sHGP to improve its solubility for polymerization. To synthesize the non-cleavable sHGP diblock copolymers (*b*-sHGP), we took the previously reported diblock poly((HPMA-*co*-PDSMA)(HPMA-*co*-MaAhxK10)) and reduced the disulfide moieties using dithiothreitol (DTT). Free sulfhydryl groups in the polymers were then conjugated to maleimide-functionalized sHGP peptide in acetononitrile/PBS solvent mixture (Scheme 1B). The control statistical copolymer of HPMA and MaAhxK<sub>10</sub>, pHK<sub>10</sub>, was used as a control material.

The sHGP-conjugated diblock copolymers (*b*-sHGP) contained about 5 sHGP per polymer based on the tryptophan absorbance at 280 nm. All polymers were further characterized by gel permeation chromatography (GPC) and amino acid analysis (AAA) for polymer dispersity and peptide incorporation (Table 1). Interestingly, the diblock copolymers showed an early elution time suggesting the formation of a higher self-assembled structure (data not shown). Equimolar solutions of sHGP-modified diblock and statistical copolymers were therefore characterized by transmission electron microscopy (TEM) and dynamic light scattering (DLS) analysis. No particles were detected by either method for statistical copolymer solutions. In contrast, TEM revealed nanoparticle structures in the diblock solutions (Fig 1A). The majority of particles were ~ 10–20 nm in diameter, although a small population of 50–100 nm particles were also observed. DLS analysis reported particles with mean hydrodynamic diameter ~250 nm, skewed by the population of larger particles (data not shown).

The particle size reported by DLS for bimodal nanoparticles has been shown to be less accurate than imaging methods since the intensity of scattered light for particle with radius 'r' is proportional to  $r^{6,16}$  We evaluated the membrane lytic capability of sHGP copolymers, pHK10, and PEI using an erythrocyte leakage assay (Figure 1B). The statistical sHGP showed a higher lytic ability at increasing polymer concentration  $(0.8-40~\mu g/mL)$  compared to the diblock analog, while the two control polymers pHK10 (a copolymer of HPMA and MaAhxK10) and polyethylenimine (PEI) showed no lytic activity at the tested concentrations. These results led us to propose that the amphiphilic diblock copolymers that contain a hydrophobic sHGP block and a hydrophilic oligolysine block, form micellar structures in aqueous solutions, thereby sequestering the lytic peptide (Figure 2).

Block copolymers, peptide, proteins and lipids, containing hydrophobic and hydrophilic segments, are known monomers that can undergo self-assembly. In the controlled release

field, self-assembled macromolecules have been utilized as constructs for drug delivery. Materials that undergo desolvation, collapse and intermolecular hydrophobic interactions can potentially form self- assembled structures such as micelles, vesicles, lamellar sheets and networks. <sup>17,18</sup> Micelle constructs are commonly formed from block copolymers, wherein assembly of hydrophobic blocks results into a hydrophobic core shielded by the hydrophilic groups. Inverted micelles, with a hydrophilic outer shell and a polycationic inner core that interacts with the negatively charged nucleic acid, have been widely exploited in plasmid delivery. <sup>19–23</sup> Polymeric or amphiphilic peptide-based micelles with a hydrophobic core and polycationic outer shell have also been reported for improved gene delivery and better cell viability. <sup>24–26</sup> Here, we evaluate a self-assembling micelle formed from an amphiphilic, peptide-polymer hybrid material for nucleic acid delivery.

The polymers were then complexed with plasmid DNA to form polyplexes with diameters ~200 nm in both water and physiologic salt concentrations (Figure 2A). These observations follow our previously reported data showing that HPMA-co-oligolysine are salt stable at DP 100.<sup>11</sup> Zeta potential measurements (Figure 2A) indicate that the net surface charge for both sHGP copolymers at N/P ratio 3 and 5 are both positive (20–30 ~kV). This is necessary for efficient polyplex-mediated gene delivery in which the excess positive charge interacts with the negatively charged cellular membrane allowing for enhanced uptake and delivery.<sup>27</sup> TEM images at N/P ratio = 5 for both copolymers complexed with DNA showed short rods (*st*-sHGP) and spherical (*b*-sHGP) morphologies (Figure 2B). Gel retardation assay demonstrated that both copolymers completely associate with plasmid DNA at a similar polymer concentration (N/P ratio = 0.5) (Figure 2C).

The complexes were then used to transfect cultured mammalian cells. *In vitro* gene transfection showed that both the diblock and statistical copolymers show similar transfection efficiency that is significantly increased over the control pHK10 copolymer; both block and statistical sHGP produced about two orders of magnitude higher reporter protein activity compared to pHK10 at N/P ratio = 3 and about an order of magnitude higher at a higher polymer concentration (N/P ratio = 5) (Figure 3). Thus the incorporation of the endosomolytic agent, sHGP, into the copolymers containing HPMA and oligolysines, further enhanced the gene delivery function of the prepared constructs, consistent with our previous report. Most notably, the diblock sHGP shows better cell viability compared to the statistical analog.

There are a few possible explanations for the increased transfection efficiency observed with the diblock copolymer. First, the sHGP may be exposed intracellularly to enhance endosomal release. While the micelles did not show lytic behavior at acidic pH (Figure 1B), other endosomal conditions, such as competitive binding to intracellular proteins, may destabilize micelles and expose sHGP. Second, micellar morphologies may themselves increase delivery efficiency. For example, Yang and coworkers previously reported that amphiphilic constructs, made up of polyalanine as the hydrophobic block and polylysine and polyhistidine as the hydrophilic block, self-assemble into cationic and micellar nanoparticles in aqueous solutions. Condensation with DNA on the outer shell demonstrated stronger DNA-binding ability and resistance to enzymatic degradation compared to the control peptide without a hydrophobic block. Most importantly, increased cell viability and transfection efficiency were observed with these micellar structures. The mechanism of increased delivery efficiency will be explored in future work.

In this communication, we have shown that the lytic activity of the truncated HGP further enhanced the gene delivery properties of the copolymers HPMA and oligolysines. Furthermore, we have demonstrated (for the first time) that peptide-based copolymers constructed in a diblock architecture, with the hydrophobic sHGP on one block and

hydrophilic oligolysine on the other, is capable of self-assembly. This is an attractive feature for designing biocompatible and non-toxic non-viral vectors for nucleic acid delivery.

## **Supplementary Material**

Refer to Web version on PubMed Central for supplementary material.

## **Acknowledgments**

The authors would like to acknowledge Dr. Russell Johnson and David Chu for their insights and helpful discussions, Profs. Anthony Convertine and Patrick Stayton for generously providing the ECT chain transfer agent and macroCTA,

#### **Funding Sources**

This work was funded by NIH/NINDS 1R01NS064404 and NSF DMR 1206426. JAP was supported by a Mary Gates Undergraduate Research Fellowship and JS was supported by an NSF graduate research fellowship under grant DGE-0718124.

#### REFERENCES

- 1. Varkouhi AK, Scholte M, Storm G, Haisma HJ. J. Controlled Release. 2011; 151:220.
- 2. Behr JP. Chimia. 1997; 51:34.
- 3. Wagner E. Advanced Drug Delivery Reviews. 1999; 38:279. [PubMed: 10837761]
- 4. Wolfert MA, Seymour LW. Gene Ther. 1998; 5:409. [PubMed: 9614562]
- 5. Hoyer J, Neundorf I. Acc. Chem. Res. 2012; 45:1048. [PubMed: 22455499]
- 6. Costin JM, Rausch JM, Garry RF, Wimley WC. Virol J. 2007; 4:123. [PubMed: 18028545]
- 7. Kwon EJ, Bergen JM, Pun SH. Bioconjugate Chem. 2008; 19:920.
- 8. Kwon EJ, Liong S, Pun SH. Mol Pharm. 2010; 7:1260. [PubMed: 20476763]
- 9. Merkel OM, Urbanics R, Bedocs P, Rozsnyay Z, Rosivall L, Toth M, Kissel T, Szebeni J. Biomaterials. 2011; 32:4936. [PubMed: 21459440]
- Ogris M, Brunner S, Schuller S, Kircheis R, Wagner E. Gene Ther. 1999; 6:595. [PubMed: 10476219]
- 11. Johnson RN, Chu DS, Shi J, Schellinger JG, Carlson PM, Pun SH. J. Controlled Release. 2011; 155:303.
- 12. Schellinger JG, Pahang JA, Johnson RN, Chu DS, Sellers DL, Maris DO, Convertine AJ, Stayton PS, Horner PJ, Pun SH. Biomaterials. 2013; 34:2318. [PubMed: 23261217]
- 13. Shi J, Schellinger JG, Johnson RN, Choi JL, Chou B, Anghel EL, Pun SH. Biomacromolecules. 2013
- Chu DS, Schellinger JG, Shi J, Convertine AJ, Stayton PS, Pun SH. Acc. Chem. Res. 2012;
   45:1089. [PubMed: 22242774]
- 15. Ahmed M, Narain R. Prog. Polym. Sci. 2013; 38:767.
- 16. Hoo CM, Starostin N, West P, Mecartney ML. J. Nanopart. Res. 2008; 10:89.
- 17. Branco MC, Schneider JP. Acta Biomater. 2009; 5:817. [PubMed: 19010748]
- 18. Chen S, Cheng SX, Zhuo RX. Macromol Biosci. 2011; 11:576. [PubMed: 21188686]
- 19. Harada-Shiba M, Yamauchi K, Harada A, Takamisawa I, Shimokado K, Kataoka K. Gene Ther. 2002; 9:407. [PubMed: 11960317]
- 20. Miyata K, Fukushima S, Nishiyama N, Yamasaki Y, Kataoka K. J Control Release. 2007; 122:252. [PubMed: 17643543]
- 21. Wei H, Volpatti LR, Sellers DL, Maris DO, Andrews IW, Hemphill AS, Chan LW, Chu DS, Horner PJ, Pun SH. Angew Chem Int Ed Engl. 2013; 52:5377. [PubMed: 23592572]
- 22. Wei H, Schellinger JG, Chu DS, Pun SH. J. Am. Chem. Soc. 2012; 134:16554. [PubMed: 23013485]

23. Convertine AJ, Diab C, Prieve M, Paschal A, Hoffman AS, Johnson PH, Stayton PS. Biomacromolecules. 2010

- 24. Wiradharma N, Khan M, Tong YW, Wang S, Yang YY. Adv. Funct. Mater. 2008; 18:943.
- 25. Guo XD, Tandiono F, Wiradharma N, Khor D, Tan CG, Khan M, Qian Y, Yang YY. Biomaterials. 2008; 29:4838. [PubMed: 18829102]
- 26. Seow WY, Yang YY. J Control Release. 2009; 139:40. [PubMed: 19470398]
- 27. Richard JP, Melikov K, Vives E, Ramos C, Verbeure B, Gait MJ, Chernomordik LV, Lebleu B. J Biol Chem. 2003; 278:585. [PubMed: 12411431]

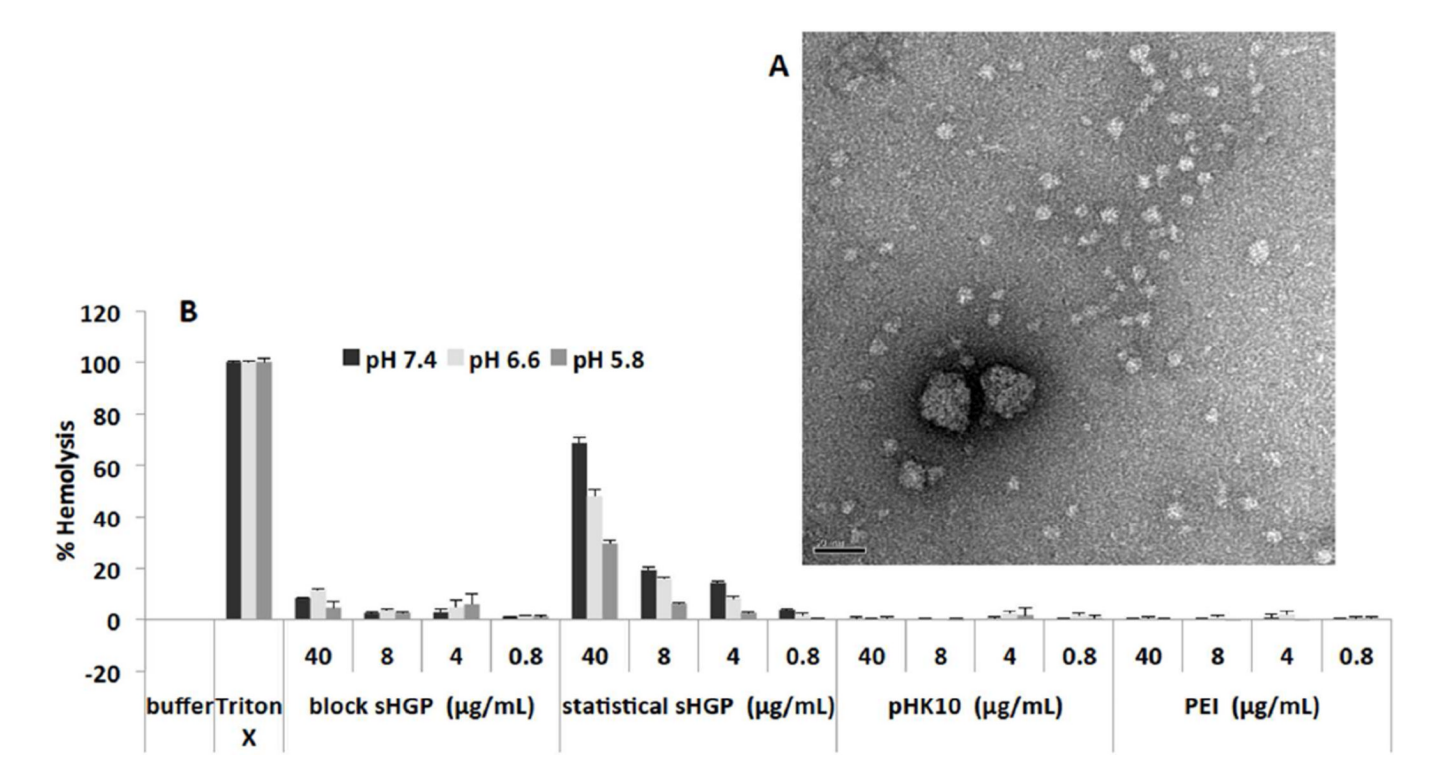
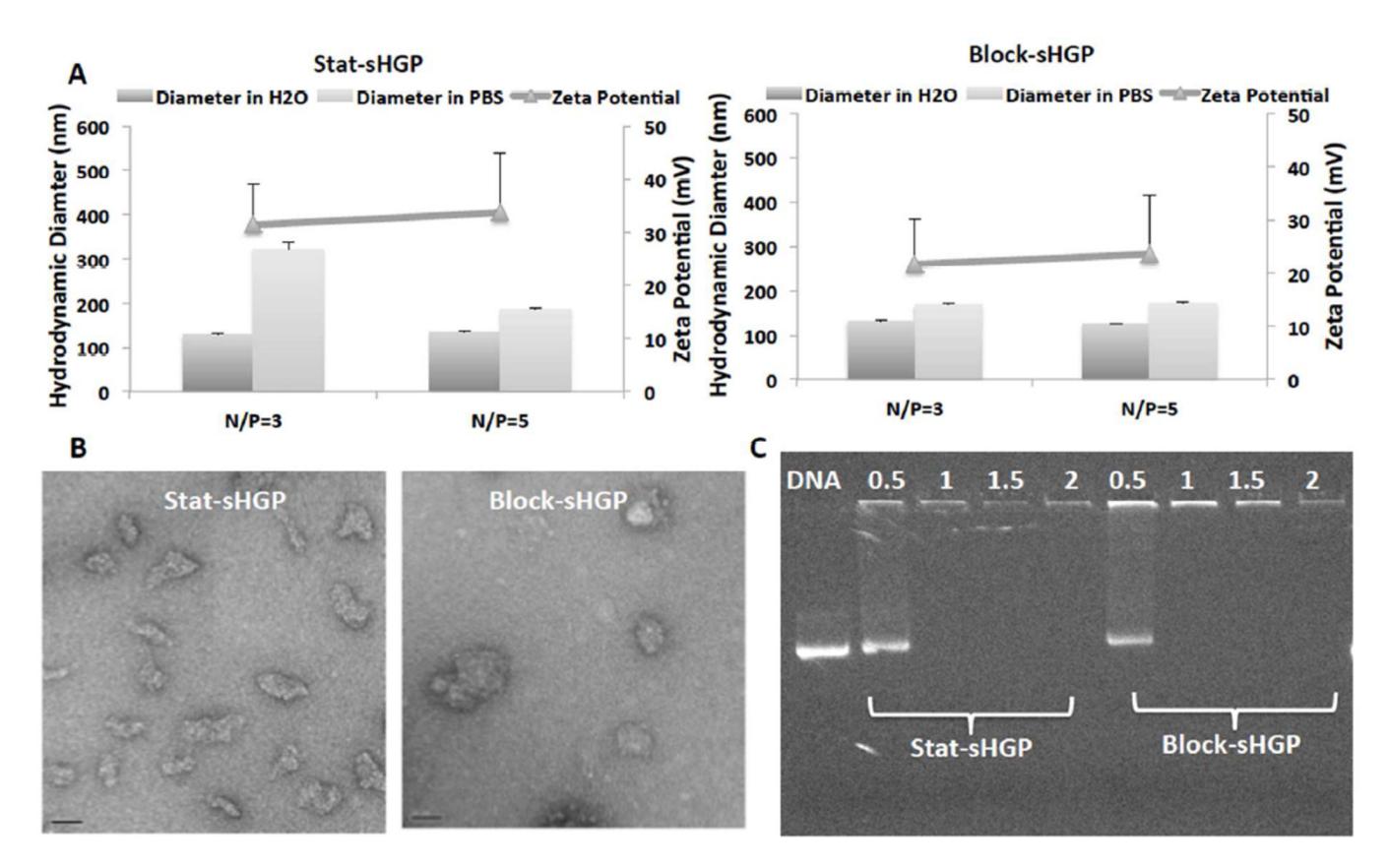


Figure 1. Characterization of block sHGP micelle. A. TEM images of block sHGP solutions in water at 40K magnification (scale bar = 50 nm) B. Hemolytic ability of polymers at various concentrations ( $\mu g/mL$ ).



**Figure 2.** Polyplex characterization. A. Sizing and zeta potential measurements of stat-sHGP and block-sHGP polyplexes at N/P ratio 3 and 5. B. TEM images of stat-sHGP and block-sHGP polyplexes. TEM images were conducted on 400-mesh formvar/copper grids stained with uranyl acetate. Scale bar represents 50 nm. C. Agarose gel electrophoresis of polymer/DNA complexes prepared at different N/P ratios using stat-sHGP and block-sHGP. Lane 1 is free DNA; lanes 2–9 correspond to N/P ratios.

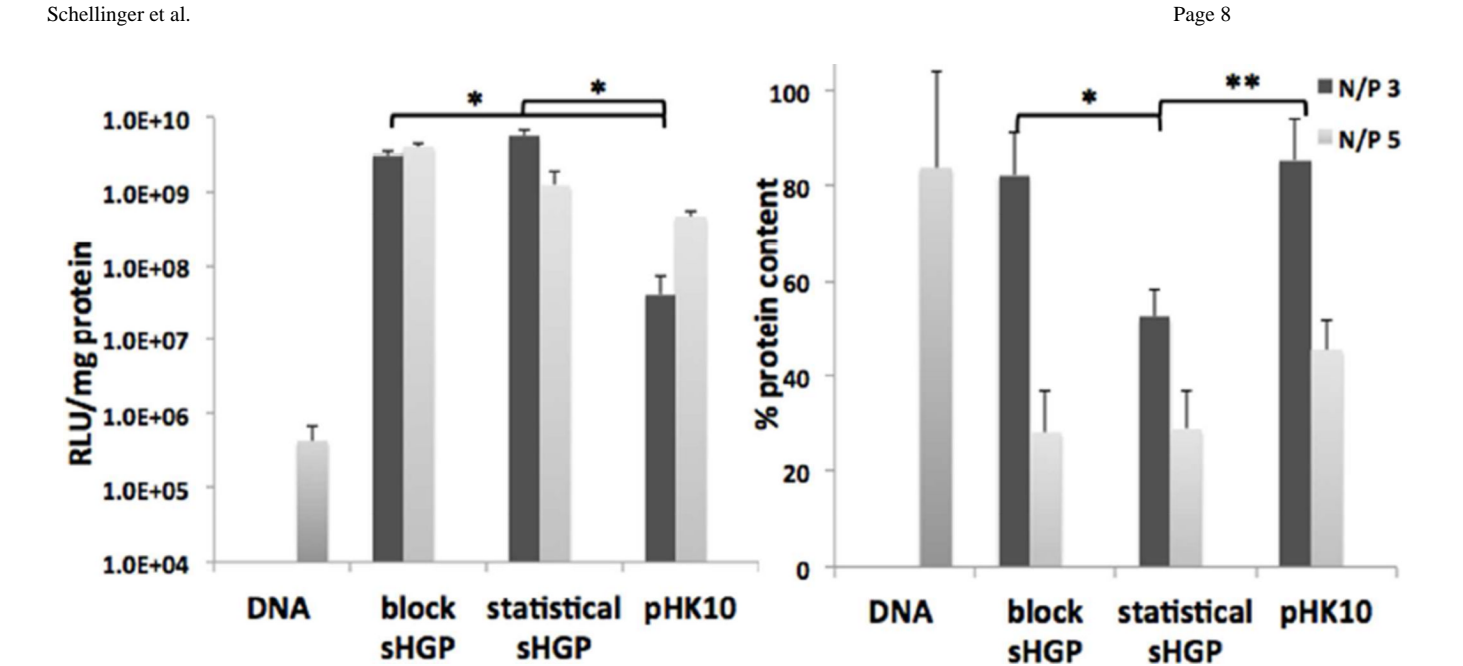
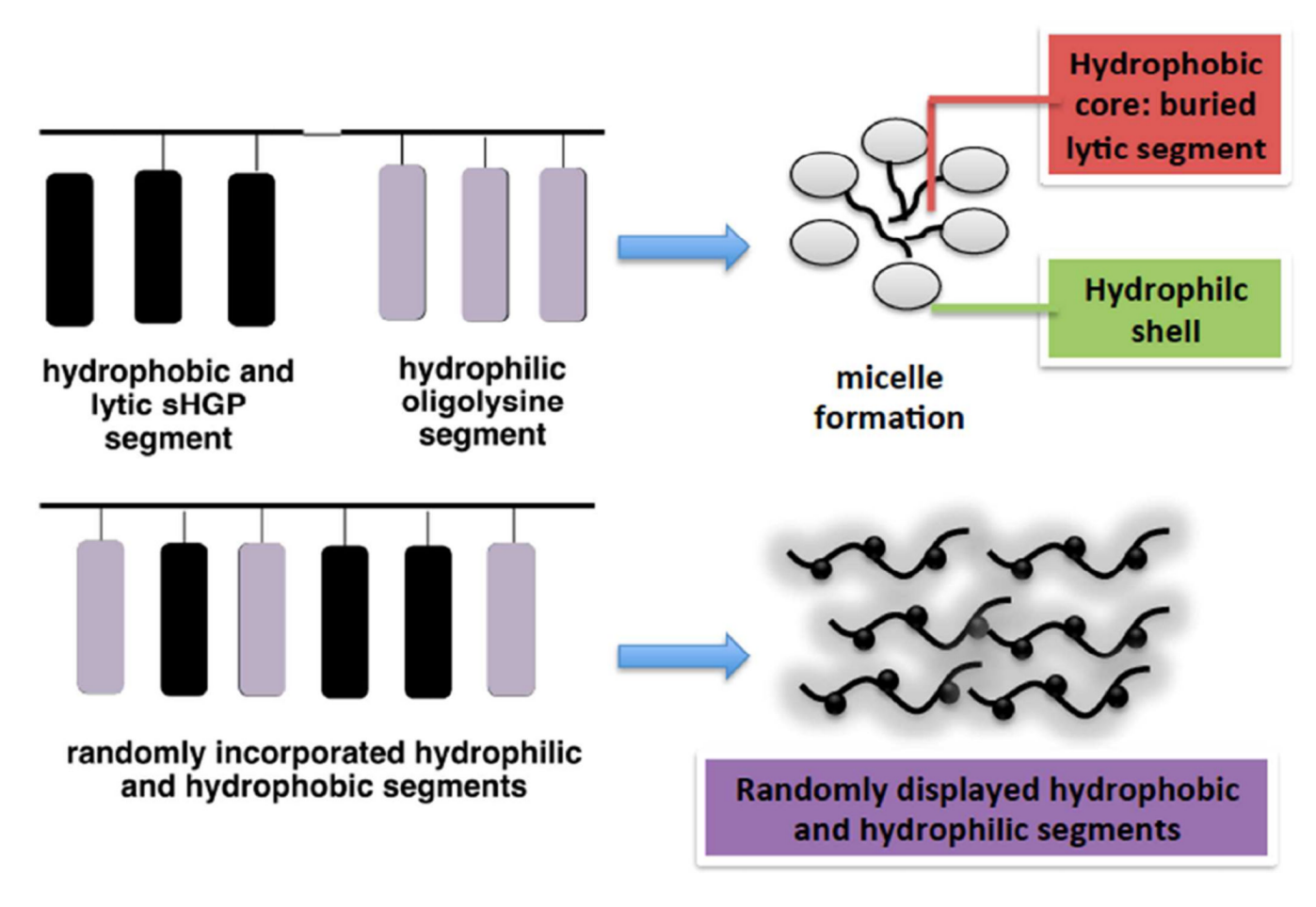


Figure 3. Transfection efficiency and cell viability of polyplexes to HeLa cells at N/P ratio 3 and 5. Data are shown as mean + SD (n = 4; student's t test, \*p<0.01, \*\*p<0.001).

#### Scheme 1.

A. Synthesis of statistical sHGP copolymers. B. Synthesis of sHGP-grafted diblock copolymers.



**Scheme 2.** Proposed polymer architecture of sHGP copolymers: Block vs. Statistical

Schellinger et al.

Table 1

Polymer characterization by GPC and AAA.

Polymer	PDI	Mn (kDa, actual)	PDI Mn (kDa, %sHGP* %K10* %HPMA* actual)	% K10*	% HPMA*
01XHADSdHHq	1.2 97	26	-	16	84
pHgsHGPbHK10 (block-sHGP)	-	-	4	10	86
pHK10sHGP (statistical-sHGP) 1.1 82	1.1	82	9	13	81

\*
relative monomer ratio analyzed by AAA

Page 11